Sādhanā Vol. 27, Part 4, August 2002, pp. 413–423. © Printed in India

Crack formation and fracture energy of normal and high strength concrete

F H WITTMANN

Centre for Durability, Maintenance and Repair, Qingdao Institute of Architecture & Engineering, Qingdao 266 033, China
Address for correspondence: Aedificat Institut Freiburg, Dunantstrasse 16, D-79110 Freiburg, Germany
e-mail: fhw@aedificat.de

Abstract. The crack path through composite materials such as concrete depends on the mechanical interaction of inclusions with the cement-based matrix. Fracture energy depends on the deviations of a real crack from an idealized crack plane. Fracture energy and strain softening of normal, high strength, and self-compacting concrete have been determined by means of the wedge splitting test. In applying the numerical model called "numerical concrete" crack formation in normal and high strength concrete is simulated. Characteristic differences of the fracture process can be outlined. Finally results obtained are applied to predict shrinkage cracking under different boundary conditions. Crack formation of high strength concrete has to be seriously controlled in order to achieve the necessary durability of concrete structures.

Keywords. Composite material; high strength concrete; fracture process; shrinkage cracking.

1. Introduction

Crack formation in concrete is often at the origin of serious damage due to corrosion. The fictitious crack model (FCM) as developed originally by Hillerborg *et al* (1976) is a powerful tool to predict crack formation in composite materials such as concrete. For a realistic prediction we need fracture energy and strain softening of the material. At present there exists a wealth of data for normal concretes, Wittmann (1995) and Mihashi & Rokugo (1998). Considerably fewer data are available for high performance concrete.

Sometimes the term high performance concrete is used for high strength concrete. In fact high performance concrete has a much wider meaning (Wittmann 1997). Strength is an important parameter among others such as ductility, self-compacting ability, low shrinkage, high modulus or wear resistance. In this contribution we will consider crack formation of high strength and normal concrete. Fracture energy and strain softening depend on the composite structure of the material. It is essentially governed by the mechanical interaction of the aggregates with the cement-based matrix. In figure 1 the influence of maximum aggregate size on the specific fracture energy is given.

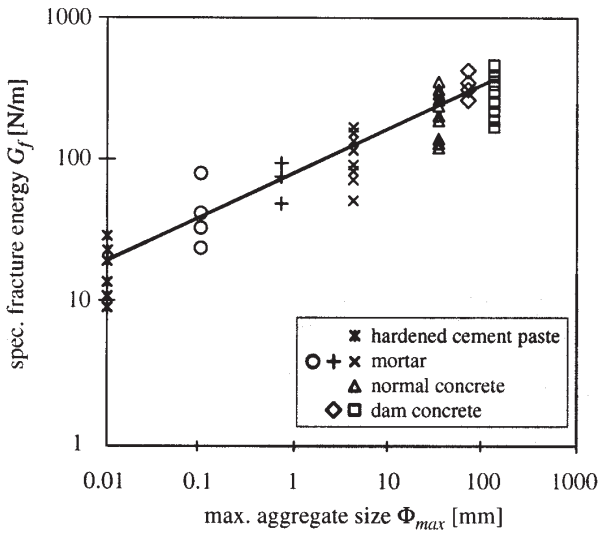

Figure 1. Specific fracture energy of cement-based materials as function of maximum aggregate size.

The lowest fracture energy is measured on pure hardened cement paste. In this case the maximum aggregate size is estimated to be 0.01 mm which corresponds to the dimensions of the remaining unhydrated clinker particles. The highest value is observed in dam concrete with a maximum aggregate size of 120 mm (Trunk & Wittmann 1998). In between the influence of maximum aggregate size on fracture energy can be described by a power function.

$$G_f = a \cdot \Phi_{\max}^n. \tag{1}$$

From the data shown in figure 1 one obtains the following values for the parameters a and n in (1): $a = 80.6$ and $n = 0.32$ (Trunk & Wittmann 1998).

In pure hardened cement paste and in fine mortar a crack can develop along a plane. The small and strong particles impose minor deviations only from an ideal fracture surface. In figure 2a a typical flat fracture surface of a mortar with a maximum aggregate size of 2 mm is shown. In figure 2b a fracture surface of normal concrete with a maximum aggregate size of 32 mm is shown. As most aggregates (river gravel) are stronger than the cement-based matrix a crack is forced to run around the inclusions. From figure 2b it can be clearly seen that a crack, once it meets an aggregate, either has to run out of the plane and leave a blank aggregate surface behind or run in the opposite direction. In the latter case, the aggregate is torn out of the matrix. The negative imprints can be seen in figure 2b.

Obviously the necessary fracture energy increases with the maximum aggregate size if the size distribution remains similar. In contrast to the energy consuming crack formation in normal concrete a crack in high strength concrete runs through the inclusions and forms approximately a plane as observed on fine mortars and pure hardened cement paste (figure 2c). In this case mechanisms of mechanical interaction between inclusions and matrix cannot be activated. This leads to the more brittle behaviour of high strength concrete. In the following we will first describe experiments to determine fracture energy and strain softening of different types of concrete. Then, by means of the well- known model "numerical concrete" (Roelfstra *et al* 1985) damage and crack formation in normal and high strength concrete will be simulated. Finally results obtained will be applied to predict shrinkage cracking under different boundary conditions.

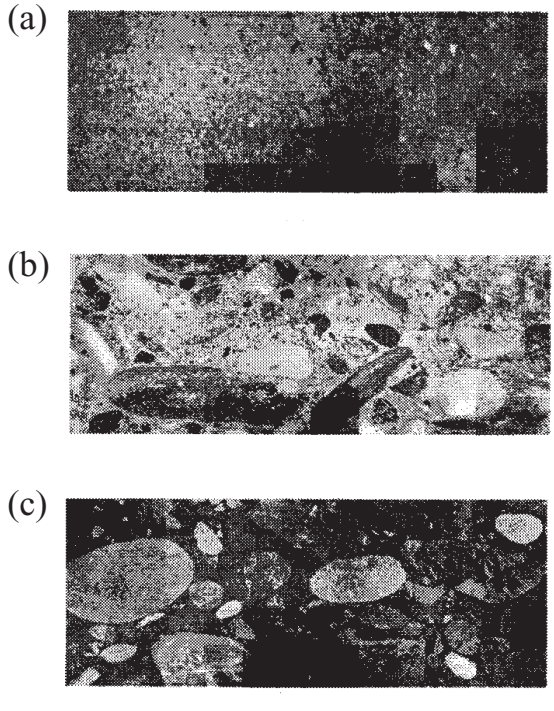

Figure 2. Fracture surface of **(a)** mortar, **(b)** normal concrete and **(c)** high strength concrete.

2. Materials and experimental results

2.1 *Concrete composition*

Three types of concrete have been produced. The mix composition is given in table 1. The maximum aggregate size has been chosen to be 32 mm for all these mixes and the size distribution follows a Fuller curve. In this way the range from a normal concrete to a high strength concrete is covered. Cubes with a side length of 150 mm and cylinders with a diameter of 150 mm have been cast.

2.2 *Experimental results*

In order to be able to simulate shrinkage crack formation a series of material parameters has to be determined. First the compressive strength and the elastic modulus have been measured

Table 1. Mix composition of the three different types of concrete.

	Mix A	Mix B	Mix C
Cement type	CEM I 425	CEM I 42,5	CEM I 52,5
Cement content (kg/m^3)	400	400	400
Water/cement ratio	0.55	0.38	0.28
Plasticizer	-	0.5 % Glenium 51	1.5 % Glenium 27
Microsilica	-	-	10%

Table 2. Compressive strength and elastic modulus at an age of 14 days.

	Mix A	Mix B	Mix C
Compressive strength (N/mm^2)	35.3	57.4	112.2
Modulus of elasticity (N/mm^2)	38,000	45,000	49,000

as function of age. The values obtained at an age of 14 days are compiled in table 2. Strength has been measured on cubes and the modulus of elasticity on cylinders.

Fracture mechanics parameters have been determined by means of the wedge splitting test (Brühwiler & Wittmann 1990). These tests have been carried out on cubes with a sawn notch having half the heigth of the cube. Results obtained are shown in figure 3. From these data strain softening can be obtained by inverse analysis. The corresponding bilinear relations are plotted in figure 4. The insert in figure 4 summarizes the parameters used in the following crack analysis. In the last line the characteristic length l_c is given as calculated by the following equation:

$$l_c = EG_f/f_t^2. \tag{2}$$

This length can be considered an indication of the brittleness of a material. In addition to the mechanical properties we also need the hygral diffusion coefficient and the shrinkage as function of relative humidity. The hygral diffusion coefficient can be calculated from measured drying data (Wittmann *et al* 1983). In figure 5, drying and shrinkage data are shown for concrete mixes A and C as examples. On this basis it is possible to calculate time-dependent moisture distributions in concrete elements prepared with the different types of concrete and under different boundary conditions in order to predict crack formation.

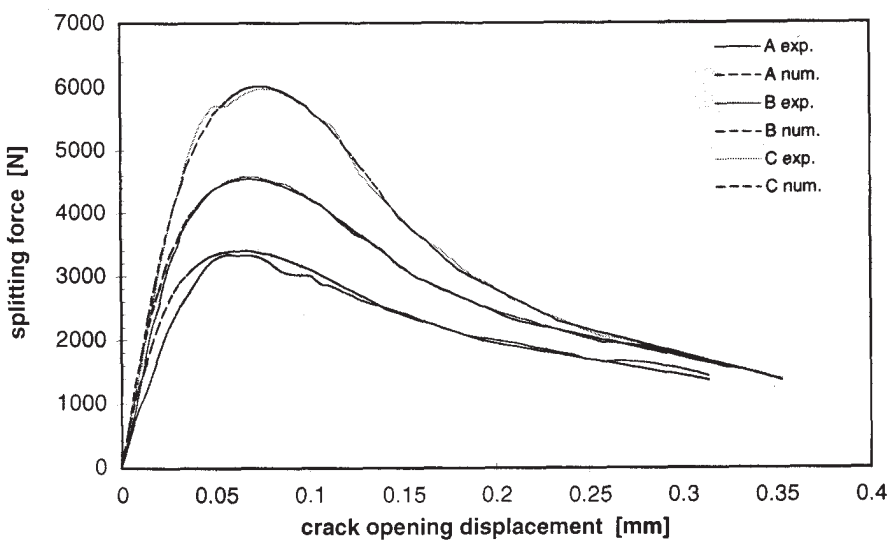

Figure 3. Results obtained by the wedge splitting test for the three types of concrete under investigation.

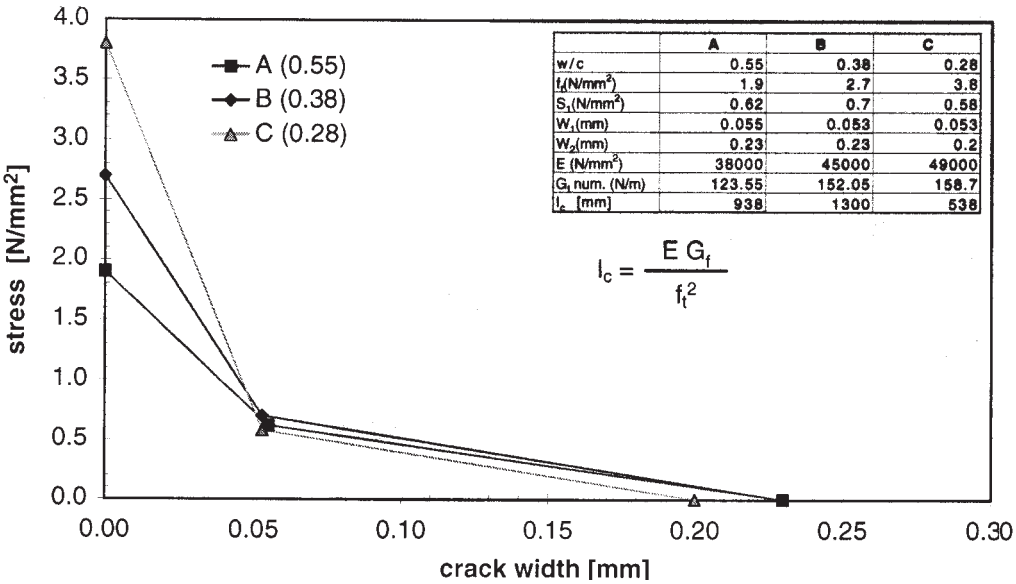

Figure 4. Bilinear relation for strain softening.

3. Numerical simulation of crack formation

In the preceeding section we have outlined how many material parameters have to be known or determined before the risk of crack formation can be realistically estimated. As a next step we will simulate numerically crack formation in a composite structure such as concrete. We consider concrete to be built up by coarse aggregates embedded in mortar matrix. In this case we need to know the material parameters of the material river gravel aggregates and the mortar with aggregates having a maximum diameter of 2 mm.

As we want to compare crack propagation through ordinary concrete and through high strength concrete we need parameters of two matrixes at least, i.e. a cement-based mortar with a w/c-ratio of about 0.5 and 0.35 respectively. Based on earlier experiments the data compiled in table 3 have been used for the numerical simulation. To simulate crack propagation a specimen used for wedge splitting experiments has been chosen. The composite structure of concrete has been simulated by generating randomly dispersed hexagonal aggregates. The size distribution of the aggregates follows a Fuller curve. The material parameters attributed to the aggregates and the two different matrixes under investigation are all given in table 3. The composite structure to be analysed is shown in figures 6 and 7.

Table 3. Material parameters used in the numerical simulation.

Materials	Aggregates	Matrix in NC	Matrix in HSC
E (GPa)	60.0	20.0	30.0
$\nu(-)$	0.2	0.2	0.2
f_t (MPa)	10.0	3.0	8.0
w_1 (mm)	0.002	0.02	0.01
σ_1 (MPa)	1.0	0.5	1.0
w_2 (mm)	0.008	0.03	0.02
G_F (N/m)	14.0	37.5	50.0

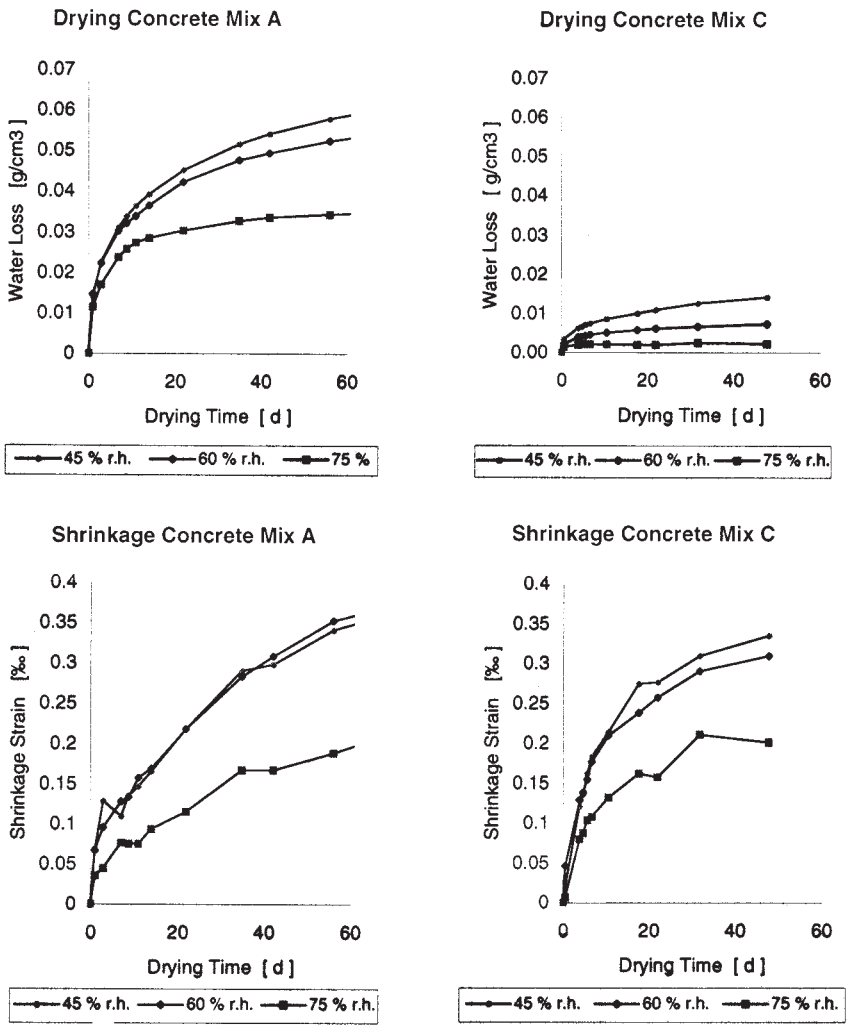

Figure 5. Drying and shrinkage data as measured on concrete mixes A and C.

If a moderate force F is applied, the system reacts linearly elastic. However, after a characteristic load is reached a fictitious crack is formed in the weaker matrix. Crack propagation in normal concrete is shown in figure 6. As the aggregates are stronger than the matrix, cracks run around the aggregates. Finally a damaged band with a width of about twice the maximum diameter of the aggregates is formed. The resulting load-crack opening diagram is shown in figure 8. It is quite clear that due to the mechanical interaction between aggregates and matrix the fracture energy of the composite material becomes considerably bigger than the fracture energy of both the aggregates and the matrix.

It should be noted at this point that the width of the damaged zone in normal concrete first increases, then remains constant as the crack runs along the ligament and finally decreases again. This means that the fracture energy is not equally distributed over the length of a crack. This phenomenon leads to a pronounced size effect (Duan *et al* 2002).

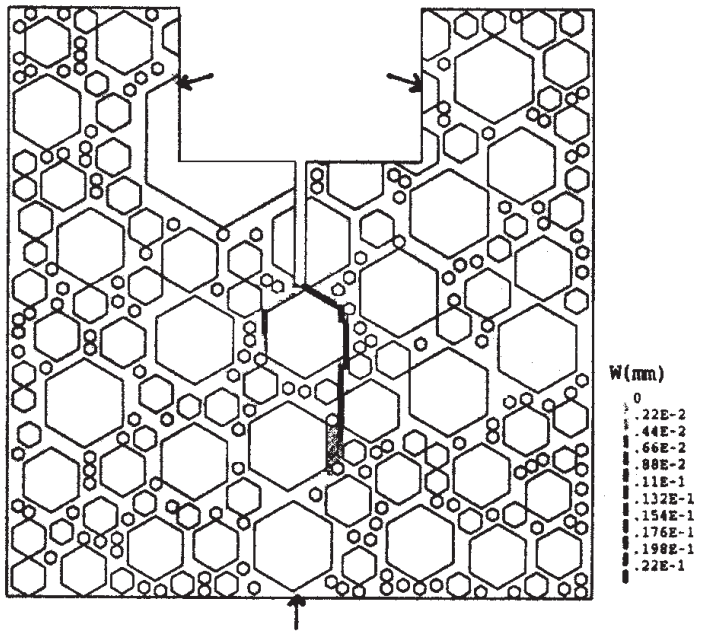

Figure 6. Damage (fictitious cracks) and crack formation in numerically simulated normal concrete.

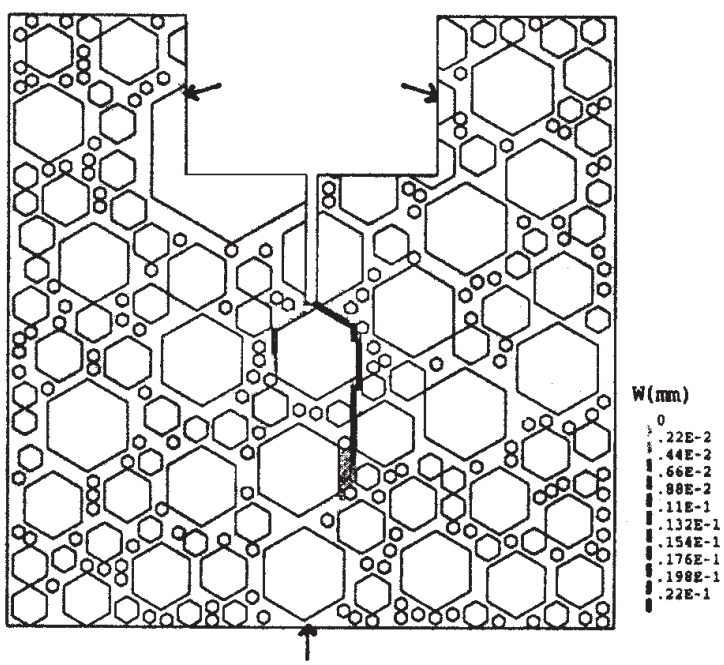

Figure 7. Damage (fictitious cracks) and crack formation in numerically simulated high strength concrete.

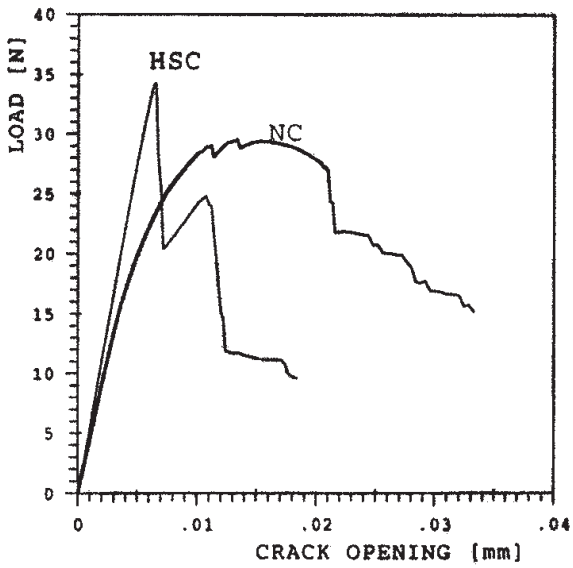

Figure 8. Load-crack opening diagram as obtained by numerical simulation for normal concrete (NC) and high strength concrete (HSC).

If crack propagation in high strength concrete is simulated, cracks can run through aggregates as the matrix and the aggregates are mechanically very similar. A typical example is shown in figure 7. A comparatively narrow crack band is formed in high strength concrete. The corresponding load-crack opening diagram is also shown in figure 8. As expected the maximum load increases but the high strength material reacts in a more brittle manner. The energy consuming mechanical interaction between aggregates and matrix is hardly activated. The results shown in figures 6 and 7 agree well with the photographs of crack surfaces as seen in figure 2.

4. Shrinkage cracking

The drying process in concrete is very slow. Hygral gradients exist for a long time in drying concrete elements with usual dimensions.

Measured shrinkage is in fact the response of a concrete specimen to the strains and stresses generated by the drying process. If the water loss of a specimen with known geometry is measured the hygral diffusion coefficient can be determined by inverse analysis, Wittmann *et al* (1983).

Time-dependent moisture distributions can then be numerically predicted. In figure 9 moisture distributions for normal concrete (mix A) and high strength concrete (mix C) are shown.

Moisture profiles in normal concrete can be realistically predicted by the general diffusion equation (Alvaredo 1994). In the case of high strength concrete a sink term has to be added to the diffusion equation because of the endogenous drying. If we compare the moisture profile after 7 days of drying for instance, the drying process affects the surface near zone in normal concrete only. In high strength concrete endogenous drying, however, leads to an equilibrium hygral potential of 0.8 in the centre of drying elements. As we will show this effect has a series of consequences with respect to crack formation. From shrinkage tests as shown in figure 5, infinitesimal shrinkage, i.e. shrinkage of an infinitesimal thin layer, can be obtained by inverse analysis (Martinola 2000). We can then attribute to each hygral potential as shown

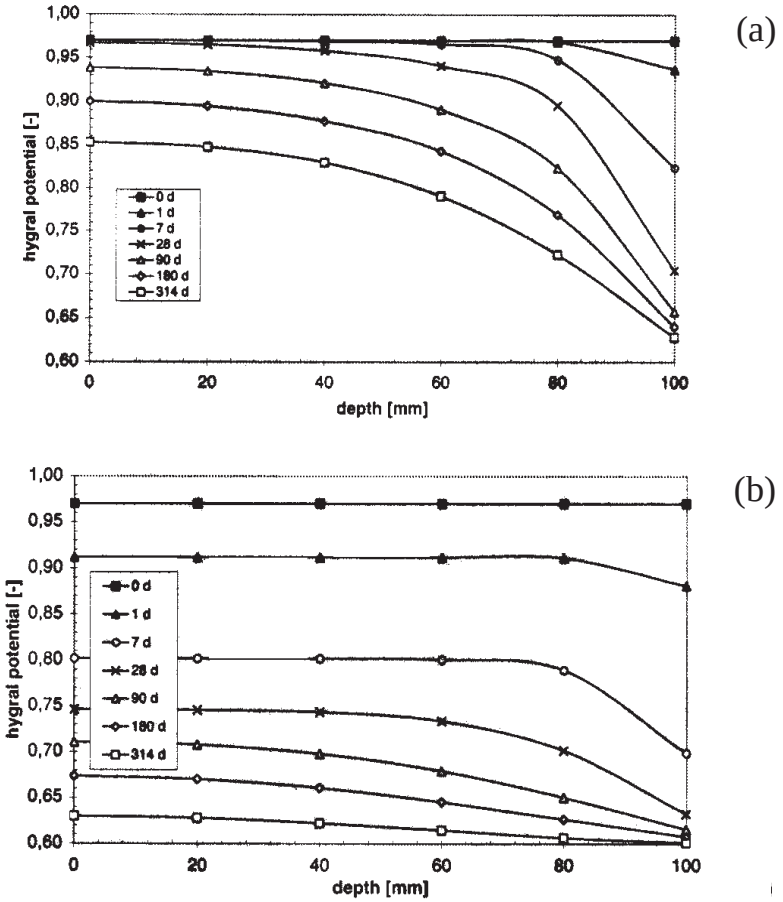

Figure 9. Moisture profiles in **(a)** normal concrete and **(b)** high strength concrete after different durations of drying

in figure 9 the corresponding infinitesimal shrinkage:

$$\varepsilon_s = \alpha(h)\Delta h. \tag{3}$$

The coefficient of infinitesimal shrinkage depends on the hygral potential (Alvaredo 1994; Martinola 2000). In order to demonstrate different crack formation in normal and high strength concrete a drying reinforced concrete beam with a length of 2 m and a height of 20 cm has been chosen as an example. For reasons of symmetry one-fourth of the beam is represented by a finite element mesh as shown in figure 10. The beam is allowed to dry through the upper and lower surface. Two boundary conditions have been chosen: (1) a free beam in which drying shrinkage can only generate eigenstresses and (2) a beam which is fully restrained at both ends.

Crack formation in reinforced beams made of normal and high strength concrete has been simulated numerically. The entering material properties such as elastic modulus, tensile strength and strain softening, hygral diffusion coefficient, coefficient of hygral dilatation have all been determined experimentally. The simulation has been carried out for the two different boundary conditions shown in figure 10.

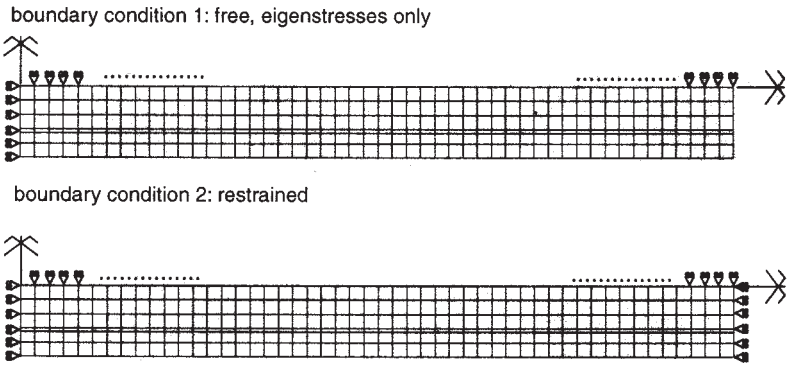

Figure 10. Finite element mesh representing one fourth of the beam to be investigated.

Results are summarised in figure 11. The free reinforced concrete beam made with normal concrete shows surface cracks only. In contrast, if this beam is fixed at both ends after a drying time of 158 days a separating crack runs through the beam. Surface cracks and the separating crack in particular have to be taken into consideration because they jeopardize long-time durability of concrete structures (see for instance Otsuki *et al* 2000).

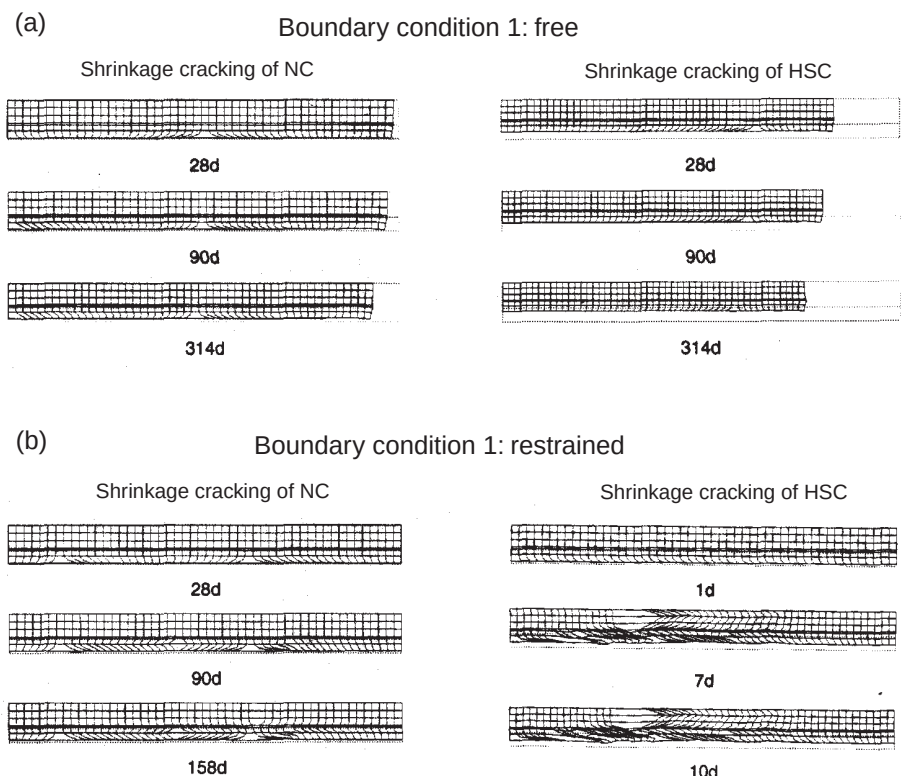

Figure 11. Crack patterns of the investigated beam made with normal concrete (NC) and high strength concrete (HSC) at different durations of drying and for two different boundary conditions. Boundary conditions **(a)** free and **(b)** restrained

The reinforced beam made with high strength concrete shows less severe surface cracking. The moisture gradients are decreased in this case by endogenous drying and shrinkage. In case the high strength concrete beam is fixed at both ends, however, a separating crack runs through the entire section after just seven days. This crack is originated by endogenous shrinkage. As endogenous shrinkage is linked to the rate of hydration it reaches critical values within a few days, while drying shrinkage is governed by slow moisture diffusion. Therefore, drying shrinkage reaches critical values after some 100 days depending on the dimensions of the drying specimen.

5. Conclusions

The following conclusions can be drawn from the results presented in this contribution.

- Crack formation and fracture energy depend on the mechanical interaction between inclusions (gravel or crushed stone) and the cement-based matrix.
- High strength means generally low ductility and increased risk for crack formation.
- A numerical model (for instance numerical concrete) can be used to optimise composite materials such as concrete with respect to well-defined requirements: strength, ductility, durability etc.
- Endogenous shrinkage takes place in high strength concrete. This process creates stress states which are not covered adequately by most codes so far.

References

Alvaredo A M 1994 Drying shrinkage and crack formation. Building Materials Reports No. 5, Aedificatio Publishers

Brühwiler E, Wittmann F H 1990 The Wedge splitting test, a new method of performing stable fracture mechanics tests. *Fracture Mech.* 35: 117–125

Duan K, Hu X, Wittmann F H 2002 A local fracture energy approach to size effect in concete fracture. *Mater. Struct.* (accepted)

Hillerborg A, Modéer M, Petersson P E 1976 Analysis of crack formation and crack growth in concrete by means of fracture mechanics and finite elements. *Cement Concrete Res.* 6: 773–782

Martinola G 2000 Rissbildung und Ablösung zementgebundener Beschichtungen auf Beton. Building Materials Reports No. 12, Aedificatio Publishers, D-Freiburg

Mihashi H, Rokugo K (eds) 1998 *Fracture mechanics of concrete structures. Proc. Third Int. Conf. of Fracture Mechanics of Concrete Structures* (D-Freiburg: Aedificatio Publ.)

Otsuki N, Miyazato S, Diola N B, Suzuki H 2000 Influences of bending crack and water-cement ratio on chloride-induced corrosion of main reinforcing bars and stirrups, *ACI Mater. J.* 97: 454–464

Roelfstra P E, Sadouki H, Wittmann F H 1985 Le béton numerique. *Mater. Struct.* 18: 327–335

Trunk B, Wittmann F H 1998 Experimental investigation into the size dependence of fracture mechanics parameters. In *Fracture mechanics of concrete structures. Proc. Third Int. Conf. of Fracture Mechanics of Concrete Structures* (eds) H Mihashi, K Rokugo (D-Freiburg: Aedificatio Publ.) vol. 3, pp. 1937–1948

Wittmann F H (ed.) 1995 Fracture mechanics of concrete structures. *Proc. Second Int. Conf. on Fracture Mechanics of Concrete Structures* (D-Freiburg: Aedificatio Publ.)

Wittmann F H (ed.) 1997 High Performance of cement-based materials. WTA report series No. 15, Aedificatio Publishers

Wittmann X H, Sadouki H, Wittmann F H 1983 Numerical evaluation of drying test data. *Transaction* 10^{th} *Conf. on Struct. Mech. in Reactor Technology* (SmiRT-10), Vol Q, pp. 71–79